Journal of King Saud University – Science 33 (2021) 101464

Contents lists available at ScienceDirect

Journal of King Saud University – Science

journal homepage: www.sciencedirect.com

Original article

Ultrasonic synthesis, XRD/HSA-interactions, DFT, time-dependence spectrophotometric stability and thermal analysis of the water-bridge {[Cu(phen)$_2$Br]Br·H$_2$O} complex

Malak Daqqa [a], Abeer A. AlObaid [b], Nabil Al-Zaqri [b,*], Firas F. Awwadi [c], Abdelkader Zarrouk [d], Ali Alsalme [b], Raghad Alasmari [b], Abdulnasser Karami [b], Ismail Warad [e,*]

[a] Department of Chemistry, Science College, An-Najah National University, P.O. Box 7, Nablus, Palestine
[b] Department of Chemistry, College of Science, King Saud University, P.O. Box 2455, Riyadh 11451, Saudi Arabia
[c] Department of Chemistry, The University of Jordan, Amman 11942, Jordan
[d] Laboratory of Materials, Nanotechnology and Environment, Mohammed V University, Faculty of Sciences, 4Av. Ibn Battuta, PO B.P., 1014 Rabat, Morocco
[e] Department of Chemistry and Earth Sciences, College of Arts and Sciences, Qatar University, P.O. Box 2713, Doha, Qatar

ARTICLE INFO

Article history:
Received 6 March 2021
Revised 13 April 2021
Accepted 29 April 2021
Available online 7 May 2021

Keywords:
Cu(II)/Phen
Dehydration
DFT
XRD
HAS
Bridge & thermal analysis

ABSTRACT

The monocationic Cu-phen mononuclear complex was assembled under ultrasonic vibration in a high yield, the presence of one water-bridge connecting both inner with outer-sphere bromides in {[Cu(phen)$_2$Br..]..H$_2$O..Br} was confirmed by XRD-crystal measurement. Moreover, the complex was analyzed by CHN-EA, FT-IR, MS, EDX, UV–Vis., and TGA. The XRD-diffraction analyses indicated the formation of distorted square pyramid [CuBr(phen)$_2$]Br·H$_2$O complex geometry, where the uncoordinated H$_2$O behaved as a bridge-molecule connecting outer-sphere Br$^-$ anion with inter-sphere one *via* two short hydrogen bonds. The thermal decomposition behavior *via* TG/DTG was also recorded. Moreover, to evaluate the complex stability over time in an aqueous medium the time-repentance spectrophotometric method was performed. The [CuBr(phen)$_2$]Br DFT/B3LYP optimized parameters and Hirschfield surface analysis (HSA) computations were matched to the experimental XRD-structural parameters and XRD-packing results respectively in order to evaluate the accuracies of the B3LYP and HSA theory levels on such complexes.

1. Introduction

The capacity of Cu(II) complexes to undergo redox processes $Cu^{2+}/Cu^{+}/Cu^{o}$ played an important role in biological applications and complexes formation (Warad et al., 2017, 2019, 2018). 1, 10-Phenanthroline is varsity bidentate *N,N*-chelating ligand, their complexes undergo stannous color changes in open atmosphere due to the different phen-coordination mode (Avdeeva et al., 2015; Youngme et al., 2007; Hu et al., 2009; Jian et al., 2001; Saleemh et al., 2017; Omoregie et al., 2015; Wesselinova et al., 2009). Several mononuclear Cu(II)-phen complexes with one/two/three phen ligands per ionic metal center with wide structures verity have been prepared (Avdeeva et al., 2015). For example, square-planar, pyramidal, octahedral and trigonal bipyramidal Cu (II) coordination geometries like in [Cu(phen)$_3$]X$_2$ (X = Cl, ClO$_4$, and BF$_4$), [Cu(phen)$_2$X]X (X = Br, I and Cl) and [CuL$_2$(phen)] (L = SCN or Br) have been prepared (Youngme et al., 2007; Hu et al., 2009; Jian et al., 2001; Saleemh et al., 2017; Omoregie et al., 2015; Wesselinova et al., 2009). A number of polynuclear complexes of Cu(II)/phen were recorded with bridging ligands like oxalate, chloride, hydroxyl and carbonate (Balboa et al., 2008; Aouad et al., 2018; Mao et al., 2001; Manna et al., 2007; Pivetta et al., 2012). Cu(I)/phen complexes support tetrahedral structure like [Cu(phen)$_2$]ClO$_4$ and trigonal geometry as in [CuX(phen)] (X = tri-t-butoxysilane thiolate or N-phtalimidate) as bulk ligand (Healy et al., 1985; Tye et al., 2008; Becker et al., 1992; Lindner et al., 1992).

The coordination ability of 1,10-phenanthroline have been openly explored by means of their structural stability during

* Corresponding author.
E-mail addresses: nalzaqri@ksu.edu.sa (N. Al-Zaqri), ismail.warad@qu.edu.qa (I. Warad).

Peer review under responsibility of King Saud University.

Production and hosting by Elsevier

https://doi.org/10.1016/j.jksus.2021.101464
1018-3647/

biochemical approaches (Tian et al., 2016; Utthra et al., 2016; Ganeshpandian et al., 2013; Ramakrishnan et al., 2009). Recently, copper-phen complexes were broadly investigated to study their interaction with DNA in order to figure out the best DNA binder and cleaver (Warad et al., 2017, 2019, 2018; Ganeshpandian et al., 2013; Ramakrishnan et al., 2009; Patel et al., 2011; Goswami et al., 2013; AL-Noaimi et al., 2014).

The thermogravimetric analysis (TGA) permitted the kinetic-parameters calculations using their TGA data gained in O_2-open or the inert atmosphere, manipulating a significant role in developing tools for mechanism estimation, moreover, TGA can supply data not only about several physical transitions but about the chemical processes (Bach and Chen, 2017; White et al., 2011; Saddawi et al., 2010; Jain et al., 2016; Burnham and Dinh, 2007; Calu et al., 2018; Lalancette et al., 2019; Zheng et al., 2019; Poornima et al., 2019; Świderski et al., 2019). Kinetic analysis of decomposition of reactions can be fruitful to understand products and intermediate behavior during their decomposition, consequently, several thermal analyses methods were developed to monitor the materials thermal behaviors (White et al., 2011); non-isothermal TG measurements methods are of an increasing significance in this field, many non-isothermal methods were expanded to achieve more kinetic-decomposition parameters (Saddawi et al., 2010; Jain et al., 2016; Burnham and Dinh, 2007). Several decomposition models were developed to estimate the kinetic reaction mechanism *via* isoconversional methods mostly using FOW or/and KAS one (Flynn and Wall, 1966a, 1966b).

Herein, the X-ray structure of mono-hydrated water-bridge molecule $[CuBr(phen)_2]Br{\cdot}H_2O$ has been prepared in a different way from the ones mentioned in Hathaway et al (Murphy et al., 1998). Since the water molecule in the structure of $[CuBr(phen)_2]H_2O.Br$ connected both counter sphere Br and internal sphere Br via two-shot H···Br hydrogen bonds, therefore it are interesting to study its TG/DTG thermal decomposition process, Moreover, the XRD-interactions and structural parameters in $[CuBr(phen)_2]Br{\cdot}H_2O$ were compared to HSA and DFT relatives parameters.

2. Experimental section

2.1. Chemicals and instruments

The chemicals used here were buy from Aldrich; FT-IR analysis was performed on a Perkin–Elmer 621 spectrophotometer. CHN-EA was performed using Elementar Varrio EL analyzer. TG- measurements was performed using TGA STD Q500. Mass spectrum (*m/z)* was performed on Finnigan 711A (8 kV). UV/Vis spectra were recorded in H_2O using Pharmacia LKB-Biochrom 4060 spectrophotometer.

2.2. Synthesis of [CuBr(phen)2]Br·H2O complex

1.2 mmol of $CuBr_2{\cdot}2H_2O$ was resolved in 25 mL of MeOH, 2.4 mmol of solid phen ligand powered was added under ultrasound wave medium to the reaction mixture, the green color appeared synchronous to phen dissolving, brown precipitate was formed after 2 min. The precipitate was washed several times by chloroform, *n*-hexane, and MeOH to ensure the purity of $[CuBr(phen)_2]H_2O.Br$, suitable crystals were formed by slow evaporation of solvents for complex solution mother (water/MeOH) mixture over a period of 5 days.

The $[CuBr(phen)_2]Br{\cdot}H_2O$ was collected as a brown powder and with 88% yield, the m.p. found to be > 360.0 °C, FT-IR (cm^{-1}): 3414 (υ_{H2O}), 3062 ($\upsilon_{C\text{-}H}$ of phen), 1520 ($\upsilon_{N=C}$), 522 ($\upsilon_{Cu\text{-}N}$). MS (*m/z*) 503.1 M^+ due to its monocationic behavior $[CuBr(phen)_2]^+$. CHN-analysis, $C_{24}H_{18}Br_2CuN_4O$, $[CuBr(phen)_2]H_2O.Br$: Calculated: C, 47.75; H, 2.94; N, 9.22%. Found: C, 47.60; H, 3.02; N, 9.12%. UV–Vis. in H_2O: λ_{max} at: 270 nm (3.2×10^4 $M^{-1}L^{-1}$) and 705 nm (2.2×10^2 $M^{-1}L^{-1}$).

2.3. DFT, XRD and HSA collections

HSA was performed *via* CRYSTAL EXPLORER 3.1 software (Frisch et al., 2009), DFT/ B3LYP/6311G+(d,p) optimization was carried out using Gaussian 09 program (Rigaku, 2015). A suitable crystal for XRD-analysis was mounted on a glass fiber and the data were collected using an Oxford X calibur diffractometer (Mo Kα radiation, λ = 0.7107 Å). Data collection and reduction were performed using CrysAlisPro software (Sheldrick, 2008). The structure was solved by direct methods and refined by least-squares method on F2 using the SHELXTL program (Spackman and McKinnon, 2002). Data collection and refinement parameters are given in Table 1.

3. Results and discussion

3.1. Synthesis

One pot-synthesis of $[CuBr(phen)_2]^+$ complex as water soluble monocationic complex was performed under ultrasonic mode of radiation (Scheme 1). The brown $CuBr_2{\cdot}2H_2O$ color in methanol solution converted to green upon addition of the solid phen ligand. 2 min latter the complex was precipitated as a brown material, the same complex have been synthesized (Wolff et al., n.d.). The desired complex found to be soluble in water but not in alcohols. Since the structure of $[CuBr(phen)_2]H_2O.Br$ was determined where one water molecule connecting both counter sphere Br with the internal sphere Br via two H···Br hydrogen bonds, therefore it is interesting to study the XRD-structural parameters and compart it with the reported same complex (Wolff et al., n.d.). Characterized by EDX, MS, CHN-EA, FT-IR, UV–Vis., spectral analysis then computed via DFT and HSA analysis.

3.2. XRD-Crystal and DFT structure

The structure of the monocation $[CuBr(phen)_2]Br{\cdot}H_2O$ confirmed by the experimental XRD and computed *via* DFT method.

Table 1
Crystal data of $[CuBr(phen)_2]H_2O.Br$.

Empirical formula	$C_{24}H_{18}Br_2CuN_4O$	
Formula weight	601.78	
Temperature	293(2) K	
Wavelength	1.54178 Å	
Crystal system, Space group	Triclinic, P-1	
Unit cell dimensions	a = 9.8385(10) Å	α = 67.573(5)°.
	b = 11.3630(12) Å	β = 67.445(5)°.
	c = 11.8711(11) Å	γ = 72.214(6)°.
Volume	1113.06(19) $Å^3$	
Z	2	
Density (calculated)	1.796 Mg/m^3	
Absorption coefficient	5.792 mm^{-1}	
F(000)	594	
Theta range for data collection	4.23 to 64.40°.	
Index ranges	$-11 \le h \le 11$, $-11 \le k \le 13$, $-13 \le l \le 13$	
Reflections collected	10,875	
Independent reflections	3574 [R(int) = 0.0491]	
Completeness to theta = 64.40°	95.7%	
Refinement method	Full-matrix least-squares on F^2	
Data/restraints/parameters	3574/0/298	
Goodness-of-fit on F^2	1.041	
Final R indices [I > 2sigma(I)]	R1 = 0.0626, wR2 = 0.1583	
R indices (all data)	R1 = 0.0718, wR2 = 0.1679	
Extinction coefficient	0.0122(10)	
Largest diff. peak and hole	0.926 and −0.799 $e.Å^{-3}$	
CCDC	1,888,392	

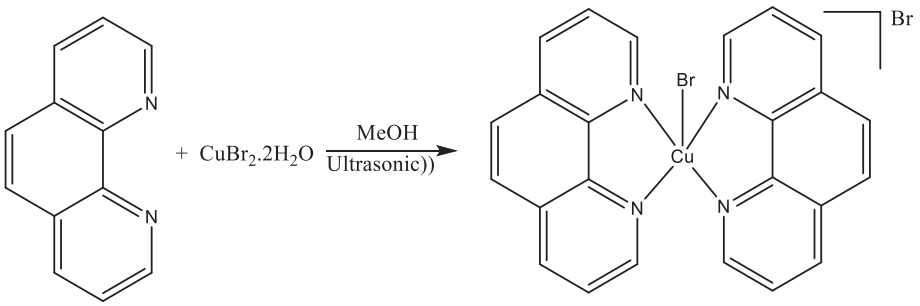

Scheme 1. Preparation of $[CuBr(phen)_2]Br{\cdot}H_2O$ complex.

The complex crystallizes as monohydrate in P-*1* space group. Uncoordinated one water molecule is connecting the outer/inter-sphere Br ions *via* two short hydrogen bonds. The Cu(II) is penta coordinated as semi-square planar *via* 4 N-atoms belong to the chelated phen ligands with τ = 45.94°, only one Br-ion occupied the axial position to complete the fifth coordination site which resulted in a distorted-square pyramidal total geometry (Fig. 1a). The DFT optimized structure was proportionated with the XRD-ORTEP solved structure (Fig. 1b). XRD-selected angles and bond lengths together with DFT-optimized structure are illustrated as in Table 2.

The structure parameters (angles and bond lengths) of $[CuBr(phen)_2]Br{\cdot}H_2O$ which was proved by XRD-single crystal measurement were matched with the optimized values obtained by DFT/B3LYP method. The DFT/exp. bond lengths graphical correlation coefficient is found to be 0.991 (Fig. 2a), meanwhile, the corresponding value of the DFT/exp. angle graphical is 0.954 (Fig. 2a). Excellent matching between calculated and experimental collected result were observed (Fig. 3c and d).

3.3. XRD-packing and HSA analysis

The presence of uncoordinated one water molecule together with one counter bromide anion attached to the Cu(II) center critically stabilized the crystal lattice *via* formation of several types of H-bonding interactions like: C-H···O, O-H···Brand C-H···Br connect totally the crystalline units within the crystalline lattice (Fig. 3a). Fig. 3b shows that the water molecule behaves as bridging-molecule, it links the complex with its counter bromide anion by two short H-bonds as: complex-Br···.H-OH with 2.298 Å and complex-Br-HO-H···.Br(counter) with 2.750 Å. More-

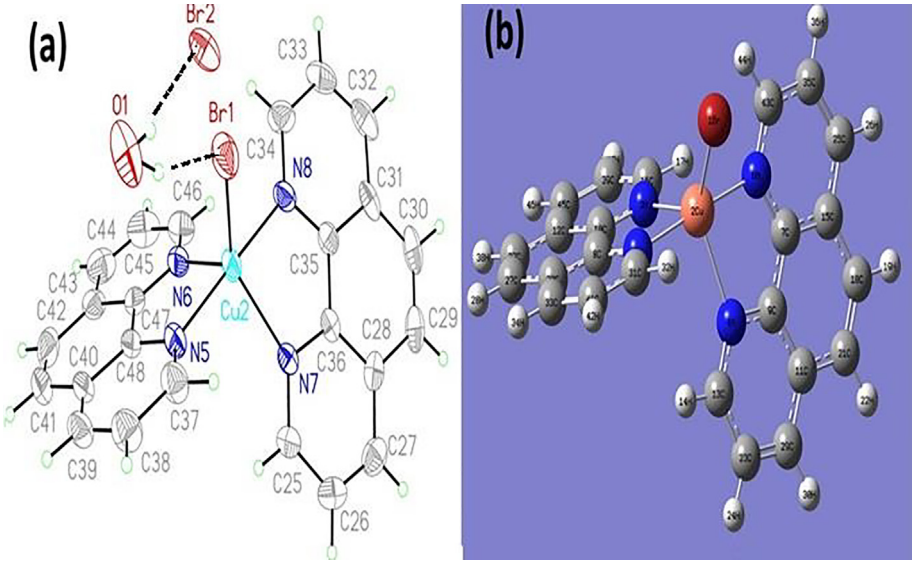

Fig. 1. $[Cu(phen)_2Br]Br$ structure, (a) the ORTEP diagram and (b) DFT optimized structure.

Table 2
XRD/exp. selected angles (°) and bond lengths (Å) compared to the DFT-result.

Bond No.	Bonds		DFT	Exp. XRD	Angles No.	Angles			Exp. XRD	DFT
1	Br1	Cu2	2.4931	2.4691	1	Br1	Cu2	N4	119.8	130.42
2	Cu2	N4	2.1227	2.087	2	Br1	Cu2	N5	126.3	130.45
3	Cu2	N5	2.0473	2.075	3	Br1	Cu2	N6	90.7	91.91
4	Cu2	N3	2.1227	1.989	4	Br1	Cu2	N7	91.5	91.92
5	Cu2	N6	2.0474	1.985	5	N4	Cu2	N5	113.9	99.13
6	N3	C10	1.3587	1.344	6	N4	Cu2	N6	81.6	78.84
7	N3	C16	1.3288	1.327	7	N4	Cu2	N7	97	98.63
8	N4	C9	1.3587	1.361	8	N5	Cu2	N6	97	98.64
9	N4	C13	1.3287	1.323	9	N5	Cu2	N7	81.9	78.85
10	N5	C8	1.3618	1.359	10	N6	Cu2	N7	177.7	176.17

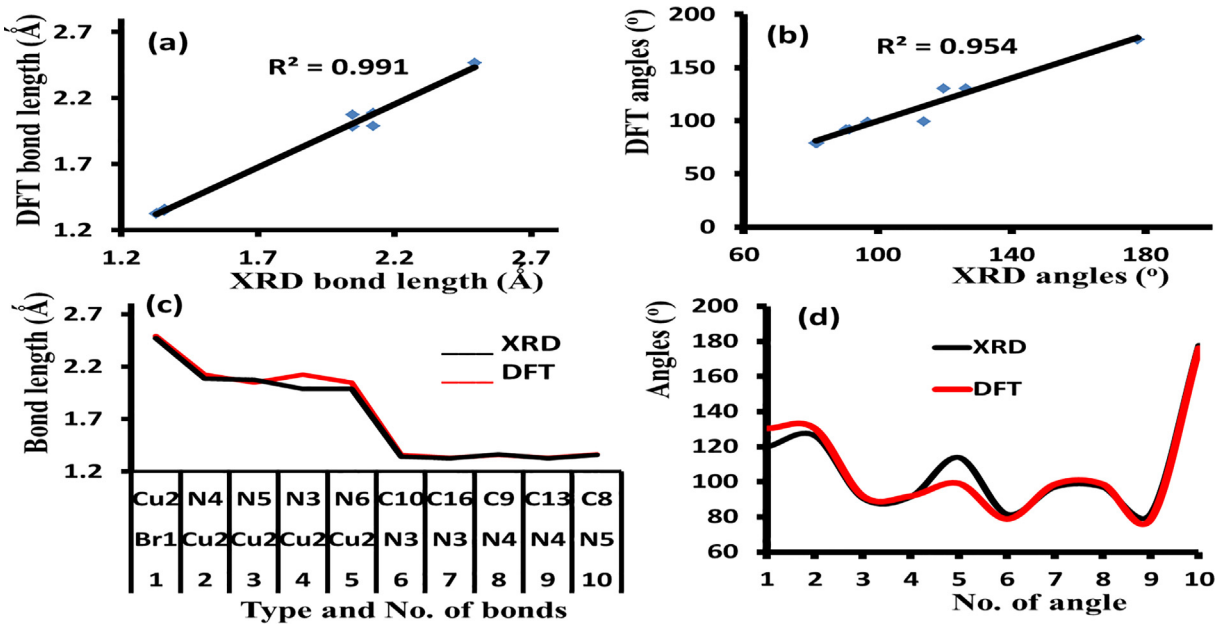

Fig. 2. (a) DFT/XRD bond distances graphical correlation, (b) DFT/XRD angles graphical correlation, (c) Histogram of DFT/XRD bond lengths and (d) Histogram of XRD/DFT angles.

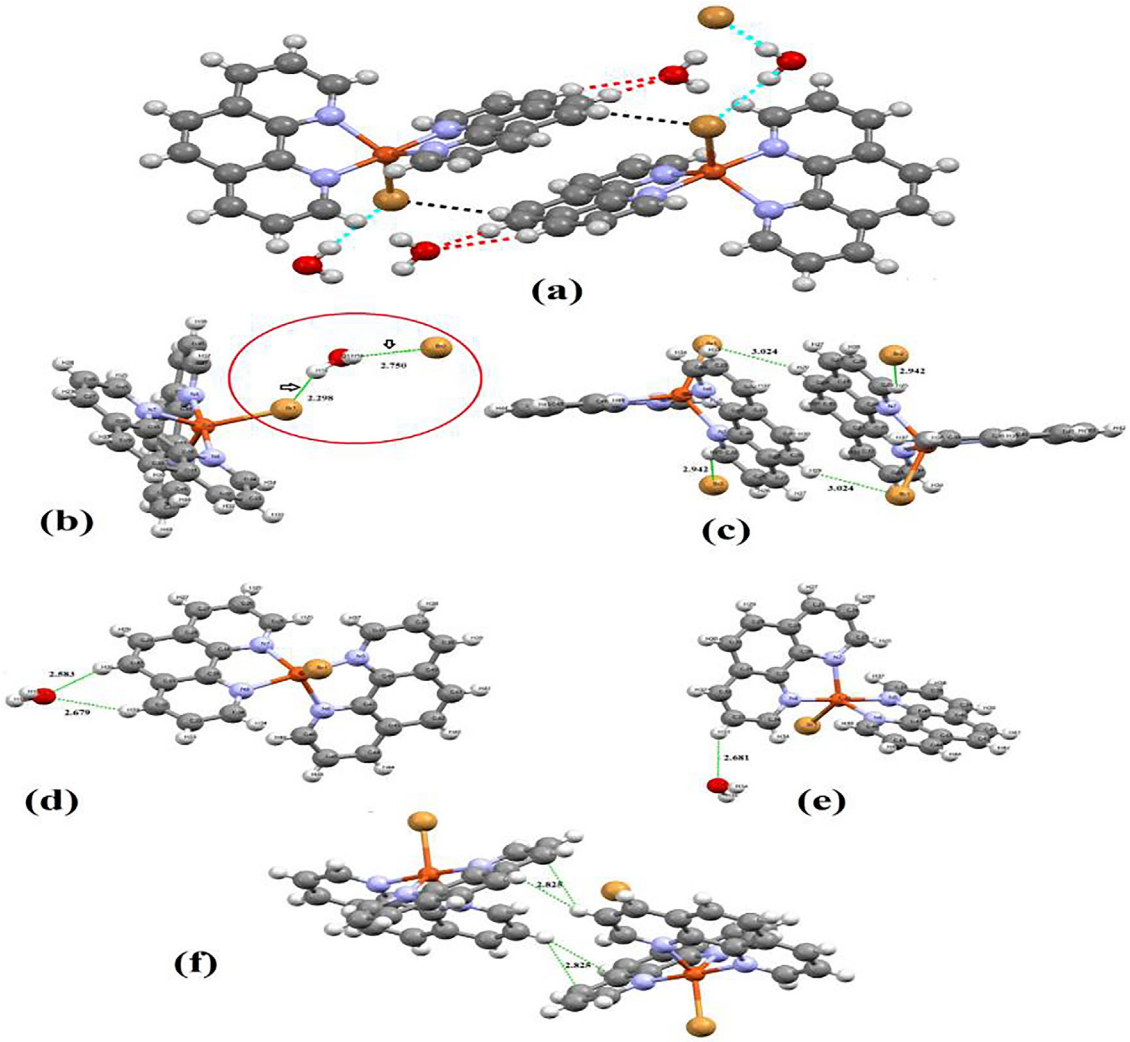

Fig. 3. All the interactions types and lengths in $[CuBr(phen)_2]Br{\cdot}H_2O$ complex.

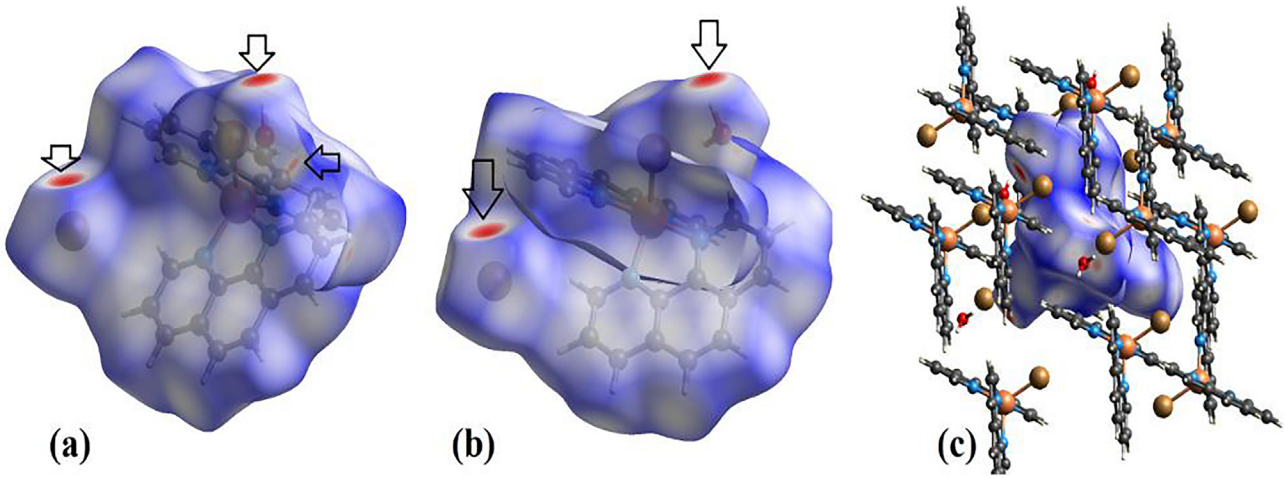

Fig. 4. d_{norm} and HSA packing plots for $[CuBr(phen)_2]Br{\cdot}H_2O$ complex.

over, two new H···.Br hydrogen bonds dimerized the complex *via* complex-Br···H_{ph} with 3.024 Å and H_{ph}···Br(counter) with 2.942 Å, as detected in Fig. 3c, the O-atom in the water molecule form another two short H-bonds, S6-form was established when O-water was binding to two terminals H_{phen} atoms with 2.583 and 2.679 Å, as seen in Fig. 3d, another H-bond was detected when O-water binding to H_{py} atom with 2.681 Å seen Fig. 3e. Two non-hydrogen bond like, phen-H···π-phen bonds with 2.825 Å average bond lengths were detected as in Fig. 3f.

HSA is a perfect computed tool to evaluate the intermolecular forces that is supported XRD-packing lattice of solved structures (Aouad et al., 2018, 2019; Betts et al., 2014). HSA result of $[CuBr(phen)_2]Br{\cdot}H_2O$ complex confirmed the presence of 3 main red spots per molecule, as in d_{norm} surface (Fig. 4a), the biggest two spots are closed to the counter bromide anion and H_2O bridge-molecule (Fig. 4b), which revealed the building of H···Br and H···O H-bonds (Fig. 4c) compatible with the XRD-crystal lattice packed result.

4. Spectral analysis

4.1. EDX, elemental analyses, MS and molar conductivity

The atomic composition of $[CuBr(phen)_2]Br{\cdot}H_2O$ complex was supported by EDX, as see in Fig. 5. The EDX spectrum proofs the presence of Br, C, N, Cu and O-water molecule elements. The CHN-analyses of $[CuBr(phen)_2]Br{\cdot}H_2O$ is agrees with EDX spectrum and confirmed the presence of one H_2O molecule in its lattice as seen in the experimental part.

MS found $[CuBr(phen)_2]Br{\cdot}H_2O$ complex with $[M^+]$ = 503.2 *m/z*, (theoretical 503.8), which supported the monocation $[CuBr(phen)_2]^+$ formula formation. The monocation nature was also supported *via* molar conductivity, 1×10^{-3} M of $[CuBr(phen)_2]Br{\cdot}H_2O$ in water and was found to be 230 $\Omega^{-1}cm^2$ mol^{-+} at RT. These results are also consistent with the solved XRD structure data.

4.2. FT-IR investigation

The $[CuBr(phen)_2]Br{\cdot}H_2O$ FT-IR is illustrated in Fig. 6. The main stretching vibrations bands can be sited as: $\nu_{(Cu\text{-}N)}$ at 518 cm^{-1}, $\nu_{(C\text{-}H)phen}$ at 3090–3020 cm^{-1}, $\nu_{(C=N)}$ at 1562 cm^{-1} and $\nu_{(H2O)}$ at 3420 cm^{-1} which proved the existence of one H_2O in the crystal lattice as well as the XRD structure (Fig. 1).

4.3. UV–Visible and the kinetic stability spectra

In water, $[CuBr(phen)_2]Br{\cdot}H_2O$ complex shows mainly two broad absorption bands, one at λ_{max} = 275 nm (UV) with two shoulders at 224 and 293 nm that assigned to π-π electron transition in phen ligands (Fig. 7a) and the second broad band at λ_{max} = 725 nm (visible) attributed to e-transition in d-d (Fig. 7b).

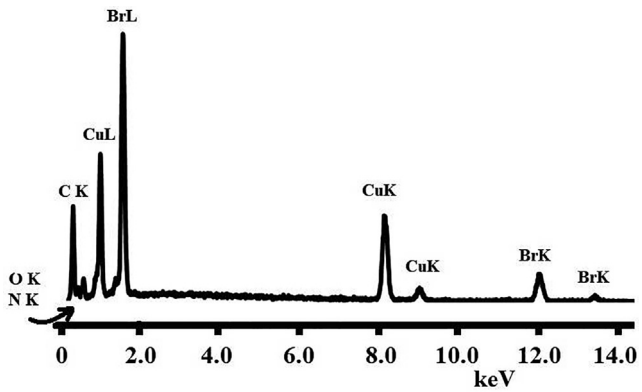

Fig. 5. EDX-spectrum of $[CuBr(phen)_2]H_2O.Br$complex.

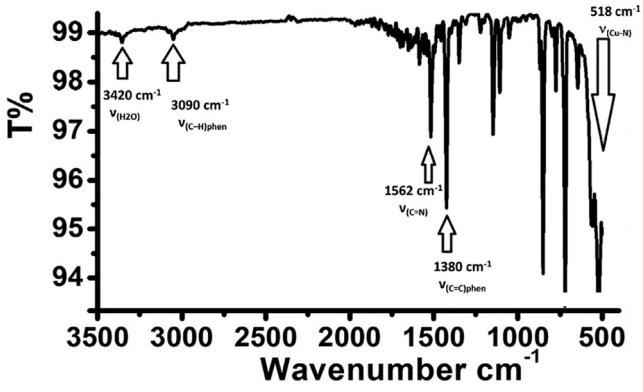

Fig. 6. FT-IR spectrum of $[CuBr(phen)_2]H_2O.Br$.

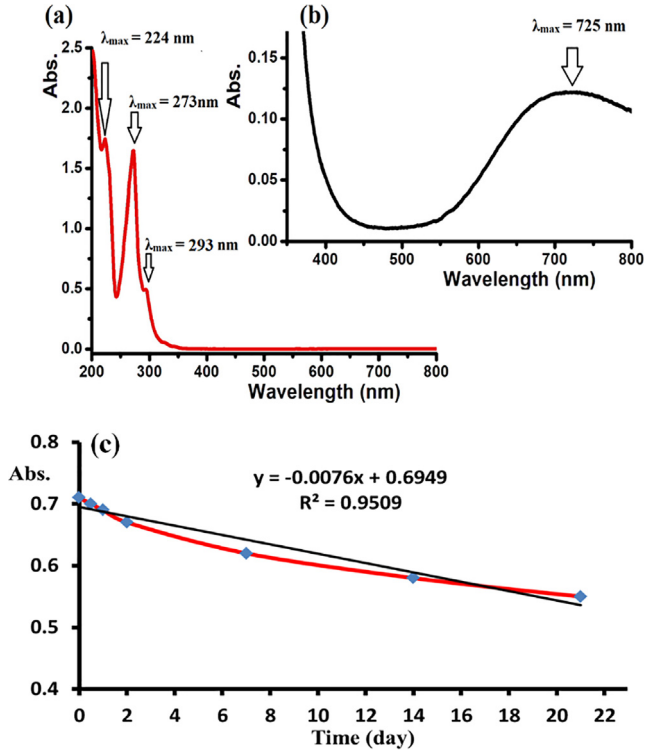

Fig. 7. At RT Abs. peaks of $[CuBr(phen)_2]Br{\cdot}H_2O$ (a) UV 1.5×10^{-4} M, (b) Vis. spectra 5.5×10^{-3} M and (c) decreased in Abs. over time at λ_{max} = 725 nm.

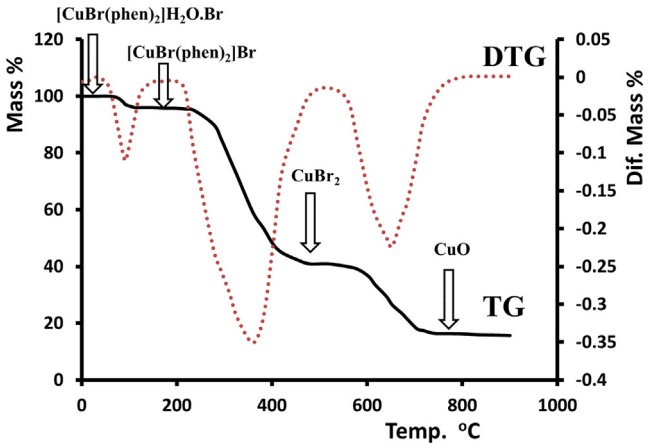

Fig. 8. TG/DTG of $[CuBr(phen)_2]Br{\cdot}H_2O$ complex.

60–110 °C, losing ~ 3.7% mass (3.9% calculated), as seen in Eq. (1), such seen is harmonic with the IR and XRD result. The phen's de-structured from $[CuBr(phen)_2]Br$ at 240–460 °C, with ~ 58.1% mass loss (59.6% calculated) where the necked $CuBr_2$ complex was prepared as a second step. The debromonation and oxidation combination reaction of $CuBr_2$ complex at 580–780 °C to produce CuO with 17.2% mass loss (16.8% calculated) is recorded as the third step.

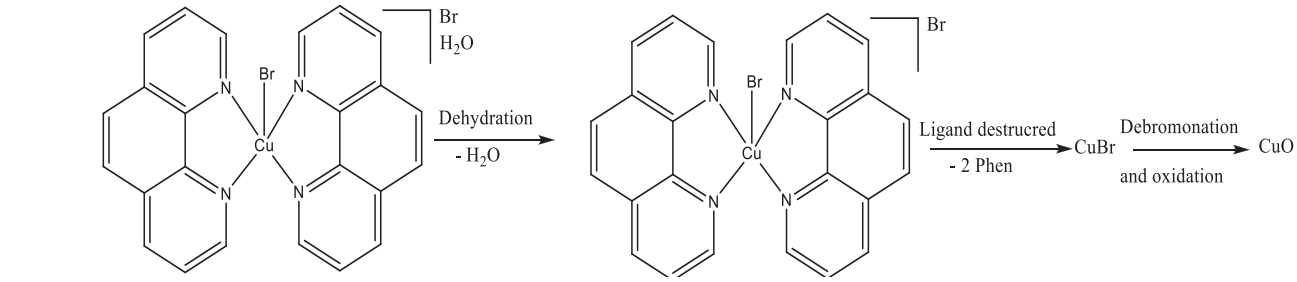

(1)

The kinetic stability of the aqueous solution of complex at ambient conditions was evaluated *via* UV/Vis. Abs. at λ_{max} = 725 nm (Fig. 7c). The spectrum indicated that the complex in aqueous solution is of good stability, no significant change in the color or the absorption of fresh dissolved sample was observed within 4 h. Moreover, in two days ~ 5% of the complex was decomposed, meanwhile, 22% of it was decomposed in 21 days, depending on the behavior of the complex observed from its linear-relationship with high graphical correlation (0.95) as in Fig. 7c, it can be estimated that, full complex decomposition needed at least around 100 days, therefore, the $[CuBr(phen)_2]^+$ is classifies as aqua-stable complex (Kumar et al., 2012; Al-Zaqri et al., 2020).

4.4. TG/DTG and isoconversional kinetics analysis

The non-isothermal TG/DTG degradation of $[CuBr(phen)_2]Br{\cdot}H_2O$ complex in air (10 °C/min. in 0 to 900 °C temperature ranges) occurred in three steps as: dehydration, de-structured and oxidation ended by CuO as final product, as seen in Fig. 8, the CuO product was confirmed by IR (Warad, 2021; Chetioui et al., 2021; Boshaala et al., 2021; Fuqha et al., 2021).

The TG/DTG three steps thermal degradation of $[CuBr(phen)_2]Br{\cdot}H_2O$ was completed at different heating rates. The dehydration of uncoordinated H_2O-bridge molecule came early as first step at

5. Conclusions

Water-soluble $[CuBr(phen)_2]Br{\cdot}H_2O$ as monocationic copper(II) complex was prepared under ultrasonic mode of radiation. The prepared complex was fully characterized *via* EDX, MS, CHN-EA, FT-IR, UV–visible and XRD analysis. The exp. XRD-crystal and the computed DFT showed a high structural compatibility as both agreed on a distorted square-pyramidal geometry bound the Cu (II) center. Moreover, the XRD-crystal solved structure indicated the formation several H-bonds, the uncoordinated H_2O bridge-molecule connected both outer/inter-sphere Br ions *via* two H-bonds. The time-repentance spectrophotometric method reflected a very stable complex in aqueous medium. TG–DTA showed $[CuBr(phen)_2]Br{\cdot}H_2O$ as a stable complex that degraded *via* dehydration, de-structured and oxidation three steps ran out to reach the CuO as stable final product. The DFT/B3LYP optimized structural parameters and the HSA of $[CuBr(phen)_2]Br$ displayed an excellent matching degree with to the experimental XRD-structural parameters and XRD-packing results respectively, to evaluate the accuracies of the B3LYP and HSA theory levels on such complexes.

Declaration of Competing Interest

The authors declare that they have no known competing financial interests or personal relationships that could have appeared to influence the work reported in this paper.

Acknowledgements

The authors extend their appreciation to the Deanship of Scientific Research, King Saud University for funding this work through research group no (RG-1440-141).

References

Al-Zaqri, N., Khatib, T., Alsalme, A., Alharthi, F.A., Zarrouk, A., Warad, I., 2020. Synthesis and amide imidic prototropic tautomerization in thiophene-2-carbohydrazide: XRD, DFT/HSA-computation, DNA-docking, TG and isoconversional kinetics via FWO and KAS models. RSC Adv. 10 (4), 2037–2048.

Aouad, M.R., Messali, M., Rezki, N., Al-Zaqri, N., Warad, I., 2018. Single proton intramigration in novel 4-phenyl-3-((4-phenyl-1H-1, 2, 3-triazol-1-yl) methyl)-1H-1, 2, 4-triazole-5 (4H)-thione: XRD-crystal interactions, physicochemical, thermal, Hirshfeld surface, DFT realization of thiol/thione tautomerism. J. Mol. Liq. 264, 621–630.

Aouad, M.R., Messali, M., Rezki, N., Said, M.A., Lentz, D., Zubaydi, L., Warad, I., 2019. Hydrophobic pocket docking, double-proton prototropic tautomerism in contradiction to single-proton transfer in thione⇔ thiol Schiff base with triazole-thione moiety: Green synthesis, XRD and DFT-analysis. J. Mol. Struct. 1180, 455–461.

Avdeeva, V.V., Dziova, A.E., Polyakova, I.N., Malinina, E.A., Goeva, L.V., Kuznetsov, N. T., 2015. Copper (I), copper (II), and heterovalent copper (I, II) complexes with 1, 10-phenanthroline and the closo-decaborate anion. Inorgan. Chim. Acta 430, 74–81.

Bach, Q.-V., Chen, W.-H., 2017. Pyrolysis characteristics and kinetics of microalgae via thermogravimetric analysis (TGA): a state-of-the-art review. Bioresour. Technol. 246, 88–100.

Balboa, S., Carballo, R., Castiñeiras, A., González-Pérez, J.M., Niclós-Gutiérrez, J., 2008. Mononuclear, dinuclear and hydroxo-bridged tetranuclear complexes from reactions of CuII ions, mandelic acid and diimine ligands. Polyhedron 27 (13), 2921–2930.

Becker, B., Wojnowski, W., Peters, K., Peters, E.-M., Schnering, H.G.V., 1992. Contributions to the chemistry of silicon-sulphur compounds—LXI. The first neutral monomeric copper (I) thiolate complex. Crystal and molecular structure of (1, 10-phenanthroline; tri-tert-butoxysilanethiolato) copper (I),[Cu {SSi (OC4H9-t) 3}(phen)]. Polyhedron 11 (6), 613–616.

Betts, H.M., Pascu, S.I., Buchard, A., Bonnitcha, P.D., Dilworth, J.R., 2014. One-pot synthesis, characterisation and kinetic stability of novel side-bridged pentaazamacrocyclic copper (II) complexes. RSC Adv. 4 (25), 12964. https://doi.org/10.1039/c3ra47450j.

Boshaala, A., Yamin, B.M., Amer, Y.O.B., Ghaith, G.S.H., Almughery, A.A., Zarrouk, A., Warad, I., 2021. Crystal interaction, Hirshfeld surface analysis, and spectral analysis of new Dithiocarbazate Schiff bases derivative (LH) and its neutral cis-Cu (L) 2 complex. J. Mol. Struct. 1224, 129207. https://doi.org/10.1016/j.molstruc.2020.129207.

Burnham, A.K., Dinh, L.N., 2007. A comparison of isoconversional and model-fitting approaches to kinetic parameter estimation and application predictions. J. Therm. Anal. Calorim. 89 (2), 479–490.

Calu, L., Badea, M., Čelan Korošin, N., Chifiriuc, M.C., Bleotu, C., Stanică, N., Silvestro, L., Maurer, M., Olar, R., 2018. Spectral, thermal and biological characterization of complexes with a Schiff base bearing triazole moiety as potential antimicrobial species. J. Therm. Anal. Calorim. 134 (3), 1839–1850.

Chetioui, S., Djedouani, A., Fellahi, Z., Djukic, J.-P., Bochet, C.G., Zarrouk, A., Warad, I., 2021. Cu (II) coordination polymer bearing diazenyl-benzoic ligand: Synthesis, physico-chemical and XRD/HSA-interactions. J. Mol. Struct. 1229, 129604. https://doi.org/10.1016/j.molstruc.2020.129604.

Flynn, J.H., Wall, L.A., 1966ab. General treatment of the thermogravimetry of polymers. J. Res. Natl. Bur. Stand. Sect. A, Phys. Chem. 70A (6), 487. https://doi.org/10.6028/jres.070A.043.

Frisch, M.J., Trucks, G.W., Schlegel, H.B., Scuseria, G.E., Robb, M.A., Cheeseman, J.R., Scalmani, G., Barone, V., Mennucci, B., Petersson, G.A., 2009. Gaussian Inc. Wallingford CT, Gaussian, p. 09.

Fuqha, M., Awwadi, F.F., Haddad, S.F., Al-Zaqri, N., Alharthi, F.A., Suleiman, M., Zarrouk, A., Boshaala, A.M., Warad, I., 2021. Design, XRD/HSA-interactions, spectral, thermal, Solvatochromism and DNA-binding of two [Cu (phen; triene)] Br 2 complexes: experimental and DFT/TD-DFT investigations. J. Mol. Struct. 1231, 129983. https://doi.org/10.1016/j.molstruc.2021.129983.

Ganeshpandian, M., Loganathan, R., Ramakrishnan, S., Riyasdeen, A., Akbarsha, M.A., Palaniandavar, M., 2013. Interaction of mixed ligand copper (II) complexes with CT DNA and BSA: effect of primary ligand hydrophobicity on DNA and protein binding and cleavage and anticancer activities. Polyhedron 52, 924–938.

Goswami, T.K., Gadadhar, S., Karande, A.A., Chakravarty, A.R., 2013. Photocytotoxic ferrocene-appended (L-tyrosine) copper (II) complexes of phenanthroline bases. Polyhedron 52, 1287–1298.

P.C. Healy L.M. Engelhardt V.A. Patrick A.H. White 12 1985 2541 10.1039/dt9850002541.

Hu, F., Yin, X., Mi, Y., Zhang, S., Luo, W., Zhuang, Y., 2009. Synthesis, structure, and properties of two novel copper (II) complexes,[Cu (phen; L) 2]· 6H2O and [Cu (phen) 3]·(ClO4) 2. Inorg. Chem. Commun. 12 (12), 1189–1192.

Jain, A.A., Mehra, A., Ranade, V.V., 2016. Processing of TGA data: analysis of isoconversional and model fitting methods. Fuel 165, 490–498.

Jian, F.-F., Lin, J.-H., Zhang, S.-S., 2001. Structure of Bischloro tris (1, 10-phenanthroline) copper (II) Dichloromethane Solvate Nonahydrate:[Cu (phen) 3] Cl2CH2Cl2· 9H2O. Chin. J. Chem. 19 (8), 772–777.

Kumar, D., Kapoor, I.P.S., Singh, G., Fröhlich, R., 2012. Preparation, characterization, and kinetics of thermolysis of nickel and copper nitrate complexes with 2, 2′-bipyridine ligand. Thermochim. Acta 545, 67–74.

Lalancette, R.A., Syzdek, D., Grebowicz, J., Arslan, E., Bernal, I., 2019. The thermal decomposition and analyses of metal tris-acetylacetonates. J. Therm. Anal. Calorim. 135 (6), 3463–3470.

Manna, S.C., Ribas, J., Zangrando, E., Ray Chaudhuri, N., 2007. Supramolecular networks of dinuclear copper (II): Synthesis, crystal structure and magnetic study. Inorgan. Chim. Acta 360 (8), 2589–2597.

Mao, Z.-W., Heinemann, F.W., Liehr, G., van Eldik, R., 2001. Complex-formation reactions of Cu (II) and Zn (II) 2, 2′-bipyridine and 1, 10-phenanthroline complexes with bicarbonate. Identification of different carbonate coordination modes. J. Chem. Soc. Dalt. Trans. 3652–3662.

AL-Noaimi, M., Choudhary, M.I., Awwadi, F.F., Talib, W.H., Hadda, T.B., Yousuf, S., Sawafta, A., Warad, I., 2014. Characterization and biological activities of two copper (II) complexes with dipropylenetriamine and diamine as ligands. Spectrochim. Acta Part A Mol. Biomol. Spectrosc. 127, 225–230.

Murphy, G., O'Sullivan, C., Murphy, B., Hathaway, B., 1998. Comparative crystallography. 5. Crystal structures, electronic properties, and structural pathways of five [Cu (phen) 2Br][Y] Complexes, Y=[Br]-⊙ H2O,[ClO4]-,[NO3]-⊙ H2O,[PF6]-, and [BPh4]-. Inorg. Chem. 37 (2), 240–248.

Omoregie, H.O., Ojattah, P., Adeleke, O.E., Woods, J.A.O., Capitelli, F., 2015. Synthesis, spectral, and antimicrobial studies of nickel (II) complexes with nitrogen-containing ligands. synth. react. inorganic. Met. Nano-Metal Chem. 45 (4), 469–476.

Patel, M.N., Gandhi, D.S., Parmar, P.A., 2011. Synthesis, biological aspects and SOD mimic activity of square pyramidal copper (II) complexes with the 3rd generation quinolone drug sparfloxacin and phenanthroline derivatives. Inorg. Chem. Commun. 14 (1), 128–132.

Pivetta, T., Isaia, F., Verani, G., Cannas, C., Serra, L., Castellano, C., Demartin, F., Pilla, F., Manca, M., Pani, A., 2012. Mixed-1, 10-phenanthroline–Cu (II) complexes: Synthesis, cytotoxic activity versus hematological and solid tumor cells and complex formation equilibria with glutathione. J. Inorg. Biochem. 114, 28–37.

Poornima, S., Premkumar, T., Butcher, R.J., Govindarajan, S., 2019. Facile one-pot template synthesis of isotypic Co (II), Ni (II) and Cu (II) complexes of a Schiff base derived from glyoxylic acid and ethyl carbazate. J. Therm. Anal. Calorim. 138 (6), 3925–3937.

Ramakrishnan, S., Rajendiran, V., Palaniandavar, M., Periasamy, V.S., Srinag, B.S., Krishnamurthy, H., Akbarsha, M.A., 2009. Induction of cell death by ternary copper (II) complexes of L-tyrosine and diimines: role of coligands on DNA binding and cleavage and anticancer activity. Inorg. Chem. 48, 1309–1322.

Rigaku, O.D., 2015. CrysAlisPro Software System, Version 1.171. 38.41 k, Rigaku Coorporation.

Saddawi, A., Jones, J.M., Williams, A., Wójtowicz, M.A., 2010. Kinetics of the thermal decomposition of biomass. Energy Fuels 24 (2), 1274–1282.

Saleemh, F.A., Musameh, S., Sawafta, A., Brandao, P., Tavares, C.J., Ferdov, S., Barakat, A., Ali, A.A., Al-Noaimi, M., Warad, I., 2017. Diethylenetriamine/diamines/copper (II) complexes [Cu (dien; NN)] Br 2: Synthesis, solvatochromism, thermal, electrochemistry, single crystal, Hirshfeld surface analysis and antibacterial activity. Arab. J. Chem. 10 (6), 845–854.

Sheldrick, G.M., 2008. A short history of SHELX. Acta Crystallogr. Sect. A Found. Crystallogr. 64 (1), 112–122.

Spackman, M.A., McKinnon, J.J., 2002. Fingerprinting intermolecular interactions in molecular crystals. CrystEngComm 4 (66), 378–392.

Świderski, G., Świsłocka, R., Łyszczek, R., Wojtulewski, S., Samsonowicz, M., Lewandowski, W., 2019. Thermal, spectroscopic, X-ray and theoretical studies of metal complexes (sodium, manganese, copper, nickel, cobalt and zinc) with pyrimidine-5-carboxylic and pyrimidine-2-carboxylic acids. J. Therm. Anal. Calorim. 138 (4), 2813–2837.

Tian, Z., huang, Y., Zhang, Y., Song, L., Qiao, Y., Xu, X., Wang, C., 2016. Spectroscopic and molecular modeling methods to study the interaction between naphthalimide-polyamine conjugates and DNA. J. Photochem. Photobiol. B Biol. 158, 1–15.

Tye, J.W., Weng, Z., Johns, A.M., Incarvito, C.D., Hartwig, J.F., 2008. Copper complexes of anionic nitrogen ligands in the amidation and imidation of aryl halides. J. Am. Chem. Soc. 130 (30), 9971–9983.

Utthra, P.P., Pravin, N., Raman, N., 2016. Scrutinizing the DNA damaging and antimicrobial abilities of triazole appended metal complexes. J. Photochem. Photobiol. B Biol. 158, 136–144.

Warad, I., 2021. One-pot ultrasonic synthesis of [Cl (N∩N') Cu (μCl) 2Cu (N∩N') Cl] dimer, DFT, XRD/HSA-interactions, spectral, Solvatochromism and TG/DTG/DSC analysis. J. Mol. Struct. 130371.

Warad, I., Awwadi, F.F., Abd Al-Ghani, B., Sawafta, A., Shivalingegowda, N., Lokanath, N.K., Mubarak, M.S., Ben Hadda, T., Zarrouk, A., Al-Rimawi, F., Odeh, A.B., Barghouthi, S.A., 2018. Ultrasound-assisted synthesis of two novel [CuBr (diamine) 2· H2O] Br complexes: Solvatochromism, crystal structure, physicochemical, Hirshfeld surface thermal, DNA/binding, antitumor and antibacterial activities. Ultrason. Sonochem. 48, 1–10.

Warad, I., Awwadi, F.F., Daqqa, M., Al Ali, A., Ababneh, T.S., AlShboul, T.M.A., Jazzazi, T.M.A., Al-Rimawi, F., Hadda, T.B., Mabkhot, Y.N., 2017. New isomeric Cu (NO2-phen) 2Br] Br complexes: Crystal structure, Hirschfeld surface, physicochemical, solvatochromism, thermal, computational and DNA-binding analysis. J. Photochem. Photobiol. B Biol. 171, 9–19.

Warad, I., Musameh, S., Sawafta, A., Brandão, P., Tavares, C.J., Zarrouk, A., Amereih, S., Al Ali, A., Shariah, R., 2019. Ultrasonic synthesis of Oct. trans-Br 2Cu (N∩ N) 2 Jahn-Teller distortion complex: XRD-properties, solvatochromism, thermal, kinetic and DNA-binding evaluations. Ultrason. Sonochem. 52, 428–436.

Wesselinova, D., Neykov, M., Kaloyanov, N., Toshkova, R., Dimitrov, G., 2009. Antitumour activity of novel 1, 10-phenanthroline and 5-amino-1, 10-phenanthroline derivatives. Eur. J. Med. Chem. 44 (6), 2720–2723.

White, J.E., Catallo, W.J., Legendre, B.L., 2011. Biomass pyrolysis kinetics: a comparative critical review with relevant agricultural residue case studies. J. Anal. Appl. Pyrolysis 91 (1), 1–33.

Wolff, S.K., Grimwood, D.J., McKinnon, J.J., Jayatilaka, D., Spackman, M.A., n.d. CrystalExplorer, University of Western Australia, Perth, Australia, 2007. Google Sch. There is no Corresp. Rec. this Ref.

Youngme, S., Wannarit, N., Pakawatchai, C., Chaichit, N., Somsook, E., Turpeinen, U., Mutikainen, I., 2007. Structural diversities and spectroscopic properties of bis and tris (1, 10-phenanthroline) copper (II) complexes. Polyhedron 26 (7), 1459–1468.

Zheng, H., Liu, X., Yin, N., Tan, Z., Shi, Q., 2019. Crystal structure, magnetic and heat capacity properties of a new chiral mononuclear iron (II) compound. J. Therm. Anal. Calorim. 135 (6), 3421–3428.